THE EFFECTS OF HEAT TRANSFER AND HYDRATE DISPERSION FORMATIONS ON THE SLUG FLOW HYDRODYNAMICS

Carlos L. Bassani[a], langebassani@gmail.com
Fausto A. A. Barbuto[a], fausto_barbuto@yahoo.ca
Amadeu K. Sum[b], asum@mines.edu
Rigoberto E. M. Morales[a], rmorales@utfpr.edu.br
[a]Multiphase Flow Research Center (NUEM), Federal University of Technology – Paraná (UTFPR), Av. Sete de Setembro, 3165, CEP 80230-901, Curitiba/PR, Brazil
[b]Chemical and Biological Engineering Department, Colorado School of Mines, 1500 Illinois St., 80401, Golden/CO, USA

Abstract. *Pipe blockage due to gas hydrate formation is a main concern to the oil and gas industry due to the costs of production impairments or interruptions. Hydrate formation scenarios are usually found in offshore production pipelines, where oil and gas flow along the pipeline as a mixture that may also contain sand and brine. The high pressure conditions and the heat transfer with the external medium – the ocean – may create the necessary conditions for hydrate formation. With this scenario in mind, the present work uses a mechanistic model to understand the effects of heat transfer and hydrate dispersion formations on the multiphase flow hydrodynamics. The model is based on the mass, momentum and energy conservation equations considering that the phases flow in the slug flow pattern – which is, incidentally, the most commonly found flow pattern in the aforementioned scenario. The simulations were carried out for a methane-water mixture flowing along a 1.5 km-length pipeline at a 10 MPa inlet pressure. Three simulation cases were run: one for isothermal flow, one with heat transfer and, lastly, one with heat transfer and hydrate formation. The discussion revolves around on how the slug flow behaves when heat transfer and hydrate formation occur, focusing on the temperature and pressure distributions, the mixture superficial velocity, the slug flow frequency and the slug flow unit cell geometry.*

Keywords*: flow assurance, hydrates, multiphase flow modeling, three-phase solid-liquid-gas slug flows, heat and mass transfer.*

1. NOMENCLATURE

Roman letters

A	Cross sectional area	[m^2]
c	Specific heat	[J/(kg.K)]
D	Diameter	[m]
dm/dt	Mass variation rate	[kg/s]
$freq$	Slug flow frequency	[Hz]
h	Heat transfer coefficient	[W/(m^2.K)]
Δh_H	Hydrate enthalpy of formation	[J/kg]
j	Phase superficial velocity	[m/s]
J	Mixture superficial velocity	[m/s]
k	Thermal conductivity	[W/(m.K)]
K	Head loss coefficient	[-]
L	Length	[m]
$\dot{m}$	Mass flow rate	[kg/s]
M	Molar mass	[kg/kmol]
P	Pressure	[Pa]
R	Phase volumetric fraction	[-]
S	Wetted perimeter	[m]
T	Temperature	[K]
T_H^{eq}	Hydrate formation equilibrium temperature	[K]
U	Real velocity	[m/s]
z	Pipe axial coordinate	[m]
Z	Compressibility factor	[-]

Greek letters

γ	Pipe inclination	[rad]
η_H	Hydration number	[-]
κ	Thermal scooping factor	[-]
μ	Viscosity	[Pa.s]
ρ	Density	[kg/m^3]
τ	Shear stress	[Pa]
ϕ	Phase ($\phi = L;G;H$)	
ψ	Slug region ($\psi = B;S$)	

Indexes

$(\bullet)_L$	Hydrate in water dispersion
B	Bubble region
eq	Equilibrium
ext	External medium
i	Gas-water interface
in	Pipe inlet
G	Gas
H	Hydrate
L	Liquid
m	Mixture
n	Node index
$ov.$	Overall
S	Slug region
sub	Subcooling
T	Unit cell translation
U	Unit cell
W	Wall

2. INTRODUCTION

Hydrates are crystals formed by the trapping of gas molecules into cages formed of hydrogen-bonded water molecules (Sloan and Koh, 2008) and high-pressure and low-temperature conditions favor their formation. Pipe blockage due to hydrate formation is one of the main challenges faced by oil and gas production companies, especially in offshore production operations in deepwater and/or cold waters (Cardoso et al., 2015). Offshore production is mainly composed by oil, gas, water (brine) and sand, where the mixture usually flows in the slug flow pattern. Slug flows are characterized by the intermittent passage of elongated bubbles, flowing over a liquid film; and liquid slug bodies, which may contain dispersed bubbles in its interior (Shoham, 2006). Together, these structures form the so-called *unit cell*.

Several approaches have been used to model slug flows, namely: stationary or quasi-stationary mechanistic models (Bassani et al., 2016b; Cook and Behnia, 2000; Shoham, 2006; Taitel and Barnea, 1990), Eulerian transient drift flux models (Danielson, 2011; Zerpa et al., 2013), Eulerian transient two-fluid models (Issa and Kempf, 2003; Simões et al., 2014), Lagrangian transient slug tracking models (Medina et al., 2015; Nydal and Banerjee, 1996; Taitel and Barnea, 1998) and hybrid models (Kjeldby et al., 2013). Fewer studies considering heat transfer (Bassani et al., 2016b; Medina et al., 2015; Simões et al., 2014; Zerpa et al., 2013) exist, but the ones considering mass transfer during hydrate formation are scarce and recent (Bassani et al., 2016a; Zerpa et al., 2013).

In this sense, the present work uses a quasi-stationary mechanistic model for gas-liquid-hydrate horizontal slug flows (Bassani et al., 2016a) to provide an explanation for the effects of heat transfer and hydrate dispersion formations on the multiphase flow hydrodynamics. Simulations for a methane and water mixture flowing along a 1.5 km-length pipeline with 10 MPa inlet pressure were carried out. Three simulation cases to evidence heat transfer and hydrate formation effects were run: one for isothermal flow, one with heat transfer and one with hydrate formation. The discussion revolves around on how the slug flow behaves when heat transfer and hydrate formation occur, focusing on the temperature and pressure distributions, the mixture superficial velocity, the slug flow frequency and the unit cell geometry.

3. MATHEMATICAL MODELING

The problem consists on characterizing gas-liquid slug flows with hydrate formation. Slug flows are defined by the intermittent passage of *unit cells* (Fig. 1a). A unit cell is composed by two defined regions ψ, the slug (*S*) and the elongated bubble (*B*). Each region may contain each phase ϕ, that is, the gas (*G*), the liquid (*L*) – herein, only water is considered –, and the hydrate (*H*). Each phase inside each region is called a *unit cell structure* $\phi\psi$.

The quasi-stationary mechanistic model that will be used herein (Bassani et al., 2016a) is based on an *Upwind Difference Scheme*, in a pipeline divided in nodes spaced by Δz (Fig. 1b). The phases' superficial velocities (j_ϕ) and the mixture pressure (*P*) and temperature (*T*) are considered known at the pipe inlet. The thermal boundary condition is an external medium with constant temperature (T_{ext}) and constant heat transfer coefficient (h_{ext}) – the ocean. A unit cell geometry model (Taitel and Barnea, 1990) is used for characterizing the elongated bubble profile and the unit cell region lengths and phase fractions. The mass balance is based on the volumetric phase fractions and is applied to find the velocities of the unit cell structures. Those velocities allow finding: (i) the structures' friction factors that are used to evaluate the pressure drop in terms of the momentum balance; and (ii) the heat transfer coefficient of each structure, used to evaluate the temperature drop by means of the energy balance. Pressure and temperature, together with the gas-water interfacial surface, are used to find the gas/water consumption and the hydrate formation rates based on a kinetic model (Turner, 2005). Thus, the superficial velocities of the phases can be recalculated node after node. The process is repeated until the end of the pipeline is reached.

The main assumptions of the model are: (i) one-dimensional, horizontal flow; (ii) incompressible liquid and real gas; (iii) Newtonian fluids; (iv) quasi-stationary mechanistic approach, (v) uniform velocity profile and constant phase fractions in each unit cell structure; (vi) constant external medium temperature as the boundary condition; (vii) negligible gas energy; (viii) negligible kinetic energy; (ix) mass transfer strictly related to hydrate formation, (x) the hydrate forms on the elongated bubble interface, forming a homogeneous hydrate-in-water dispersion.

The equations of the model are summarized on Tab. 1 and the definitions of their parameters are given in the nomenclature section. Further information can be found in Bassani et al. (2016a).

The kinetic model of Turner (2005) is used to predict the gas mass consumption rate dm_G/dt during hydrate formation by means of the gas-water interfacial surface, A_i, and the subcooling of the system, ΔT_{sub}, Eq. (1). Hydrates may form only when $\Delta T_{sub} = T_H^{eq} - T \geq 0$. Here, it is assumed that hydrates must reach a critical subcooling level before the nucleation process starts, fixed at $\Delta T_{sub,crit} \approx 3.6K$ (Matthews et al., 2000). Using the concept of hydration number η_H – that is, an averaged stoichiometry between the gas and the water for forming the hydrate, with $\eta_H \approx 6$ for sI crystalline structures (Sloan and Koh, 2008) –,the water consumption rate dm_L/dt and the hydrate formation rate dm_H/dt, Eqs. (2) and (3), can be estimated.

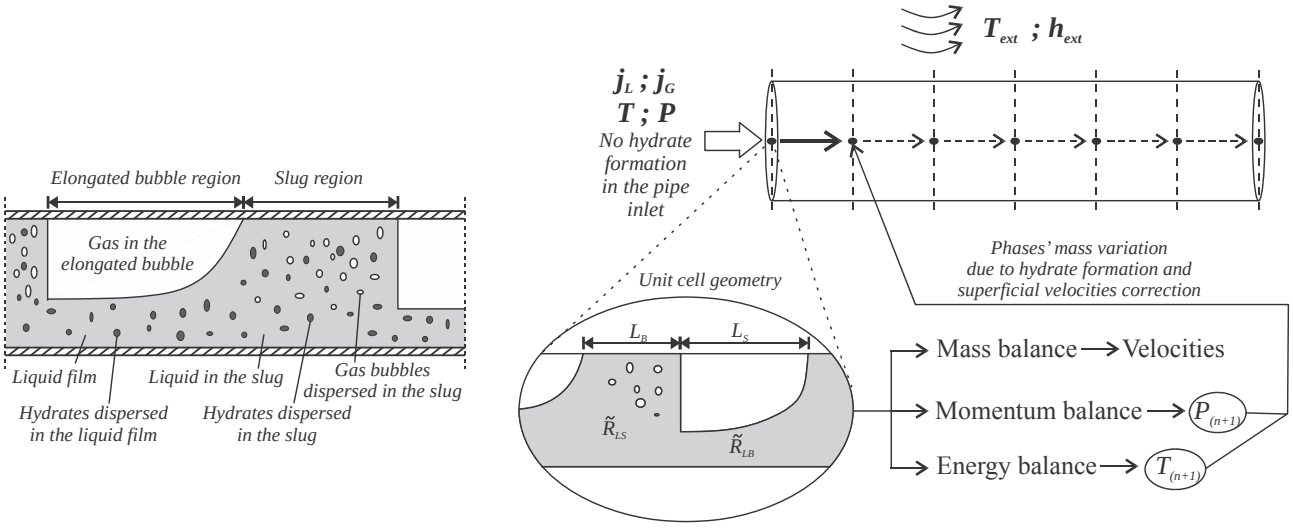

Figure 1. a) Unit cell definition and b) problem characterization.

Table 1. Equations of the model.

Description	***Equations***	***Ref.***
Phases' mass consumption/formation rate (Turner, 2005)	$\frac{dm_G}{dt} = -k_1 \exp\left(\frac{k_2}{T}\right) A_i \Delta T_{sub} \quad \frac{dm_L}{dt} = \eta_H \frac{M_L}{M_G}\frac{dm_G}{dt} \quad \frac{dm_H}{dt} = -(\eta_H + 1)\frac{M_H}{M_G}\frac{dm_G}{dt}$	(1),(2),(3)
Velocities of the unit cell structures	$\tilde{U}_{LB} = U_T + (\tilde{U}_{LS} - U_T)\frac{\tilde{R}_{LS}}{\tilde{R}_{LB}} - \frac{1}{\tilde{\rho}_L A \tilde{R}_{LB}}\left[\frac{dm_L}{dt} + \frac{dm_H}{dt}\right] \quad U_{GB} = U_T + (U_{GS} - U_T)\frac{R_{GS}}{R_{GB}} - \frac{1}{\rho_G A R_{GB}}\frac{dm_G}{dt}$	(4),(5)
Film height ODE and liquid mass conservation on the unit cell (Taitel and Barnea, 1990)	$\frac{d\tilde{H}_{LB}}{dz} = \frac{\frac{\tilde{\tau}_{LB}\tilde{S}_{LB}}{\tilde{A}_{LB}} - \frac{\tau_{GB}S_{GB}}{A_{GB}} - \tau_i S_i\left(\frac{1}{\tilde{A}_{LB}} + \frac{1}{A_{GB}}\right) + (\tilde{\rho}_L - \rho_G) g \sin\gamma}{(\tilde{\rho}_L - \rho_G) g\cos\gamma - \left(\tilde{\rho}_L \frac{\lvert U_{LB} - U_T\rvert (U_{LB} - U_T)}{\tilde{R}_{LB}} + \rho_G \frac{\lvert U_{GB} - U_T\rvert (U_{GB} - U_T)}{R_{GB}}\right)\frac{d\tilde{R}_{LB}}{d\tilde{H}_{LB}}}$ $\frac{L_U(\tilde{U}_{LS}\tilde{R}_{LS} - \tilde{j}_L)}{U_T} = L_B(R_{GB} - R_{GS})$	(6) (7)
Phases' superficial velocities correction along the pipeline	$j_{G(n)} = j_{G(n-1)}\frac{Z_{(n)}}{Z_{(n-1)}}\frac{P_{(n-1)}}{P_{(n)}}\frac{T_{(n)}}{T_{(n-1)}} + \frac{1}{\rho_G A}\frac{dm_G}{dt}\frac{\Delta z}{L_U} \quad j_{L(n)} = j_{L(n-1)} + \frac{1}{\rho_L A}\frac{dm_L}{dt}\frac{\Delta z}{L_U} \quad j_{H(n)} = j_{H(n-1)} + \frac{1}{\rho_H A}\frac{dm_H}{dt}\frac{\Delta z}{L_U}$	(8),(9),(10)
Hydrate and water fractions	$R_{L\psi} = \tilde{R}_{L\psi}(1 + j_H / j_L)^{-1} \quad R_{H\psi} = \tilde{R}_{L\psi}(j_H / j_L)(1 + j_H / j_L)^{-1}$	(11),(12)
Pressure distribution	$P_{(z)} = P_{in} - \left[\frac{\tilde{\tau}_{LS}S_{LS}}{A}\frac{L_S}{L_U} + \frac{(\tilde{\tau}_{LB}S_{LB} + \tau_{GB}S_{GB} + \tau_i S_i)}{A}\frac{L_B}{L_U} + K\tilde{\rho}_{LB}\frac{(\tilde{U}_{LB} - U_T)^2}{2L_U}\right] z$	(13)
Temperature distribution	$T_{(z)} = \frac{p}{n} + \left(T_{in} - \frac{p}{n}\right)\exp\left(-\frac{n}{m}z\right) \quad n = \left(\tilde{h}_{LB}\tilde{S}_{LB}L_B + \tilde{h}_{LS}\tilde{S}_{LS}L_S\right) - \dot{m}_z\tilde{c}_L\kappa + \Delta h_H k_1 A_i \exp\left(\frac{k_2}{T_{(n-1)}}\right)$ $m = \tilde{\rho}_L A \tilde{R}_{LU} U_T L_U \tilde{c}_L \quad p = \left[\left(\tilde{h}_{LB}\tilde{S}_{LB}L_B + \tilde{h}_{LS}\tilde{S}_{LS}L_S\right) - \dot{m}_z\tilde{c}_L\kappa\right]T_W + \Delta h_H k_1 A_i T_H^{eq}\exp\left(\frac{k_2}{T_{(n-1)}}\right)$ $\kappa = \exp\left(\frac{\tilde{h}_{LB}\tilde{S}_{LB}L_B}{\tilde{\rho}_L\tilde{c}_L A\tilde{R}_{LB}\tilde{U}_{LB}}\right) - \exp\left(-\frac{\tilde{h}_{LS}\tilde{S}_{LS}L_S}{\tilde{\rho}_L\tilde{c}_L\tilde{R}_{LS}A\tilde{U}_{LS}}\right) \quad \dot{m}_z = \tilde{\rho}_L\tilde{R}_{LB}A(U_T - \tilde{U}_{LB}) = \tilde{\rho}_L\tilde{R}_{LS}A(U_T - \tilde{U}_{LS})$	(14),(15) (16),(17) (18),(19)
Wall temperature	$T_W = T + \left[\frac{\tilde{h}^{ov.}_{LB}}{\tilde{h}_{LB}}\frac{L_B}{L_U} + \frac{\tilde{h}^{ov.}_{LS}}{\tilde{h}_{LS}}\frac{L_S}{L_U}\right]\frac{D}{D_{ext}}(T_{ext} - T) \quad \tilde{h}^{ov.}_{\phi\psi} = \left[\frac{D}{D_{ext}h_{ext}} + \frac{D\ln(D_{ext}/D)}{2k_W} + \frac{1}{\tilde{h}_{\phi\psi}}\right]^{-1}$	(20),(21)
Mixture heat transfer coefficient and mass flow rate	$\frac{h_m S}{\dot{m}_m\tilde{c}_L} \approx \frac{n}{m} \quad \dot{m}_m = \rho_G j_G A + \rho_L j_L A + \rho_H j_H A$	(22),(23)

The mass consumption/formation rates for each phase, Eqs. (1) to (3), are used for estimating the film and the elongated bubble velocities, Eqs. (4) and (5), when the gas and hydrate-in-water dispersion mass balances is applied to the control volume of Fig. 2a. The dispersed bubbles' velocity is considered equal to the one of the slug, $U_{GS} \approx \tilde{U}_{LS}$, an

assumption valid for horizontal flows (Harmathy, 1960). Therefore, the slug velocity is equal to the mixture superficial velocity when considering a constant mixture velocity along the unit cell (Shoham, 2006), that is, $\tilde{U}_{LS} \approx J$.

The unit cell geometry is estimated by using Taitel and Barnea's (1990) model. A mixed momentum balance between the gas and the dispersion is applied to the elongated bubble region to find and ODE for the film height $\tilde{H}_{LB}$, Eq. (6). This ODE is numerically integrated until convergence with the liquid mass balance for the entire unit cell, Eq. (7), is achieved. The bubble length and the mean gas fraction in the elongated bubble region arise from this integration process, and are expressed as $L_B = \int_0^{L_B} dz$ and $R_{GB} = 1 - \frac{1}{D}\int_0^{L_B} \frac{d\tilde{H}_{LB}}{dz} dz$, respectively. The unit cell length is the ratio between the unit cell translational velocity and the slug flow frequency, $L_U = U_T / freq$. The slug length is straightforwardly estimated as $L_S = L_U - L_B$.

Experimental correlations for the slug flow frequency (Schulkes, 2011), the unit cell translational velocity (Petalas and Aziz, 1998) and the gas fraction in the slug body (Andreussi et al., 1993) are required so that model closure can be achieved. These experimental correlations are a function of superficial velocities of the phases. In this sense, Eqs. (8) to (10) present the correction of the superficial velocities of the phases along the pipeline in terms of the mass consumption/formation rates, Eqs. (1) to (3). Pressure and temperature variations are also computed for the gas.

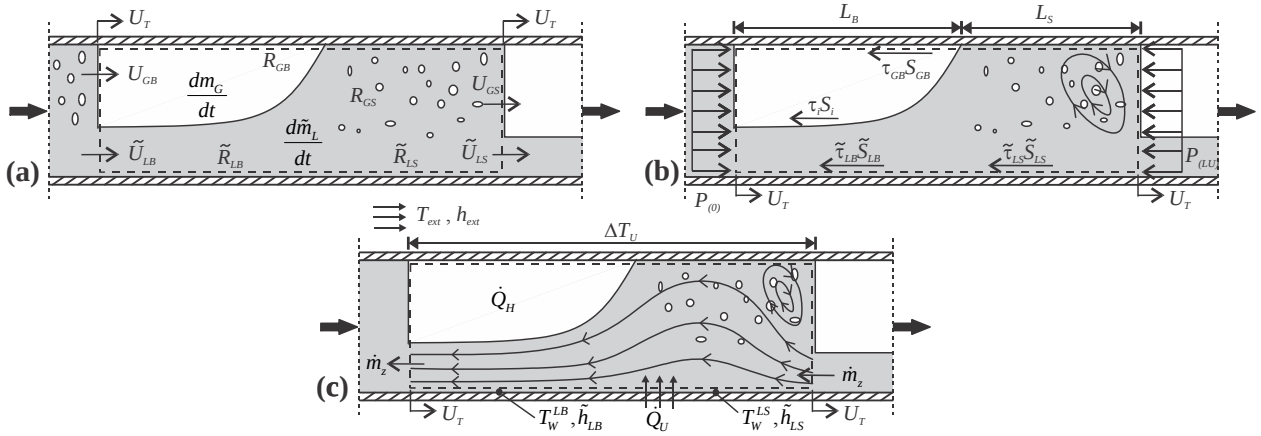

Figure 2. Control volume definitions for: a) mass, b) momentum and c) energy balances.

Thus far, the three-phase gas-water-hydrate flow was treated as a two-phase flow between the gas and the hydrate-in-water dispersion, considering that the dispersion has homogeneous properties. However, the actual hydrate and water phase fractions are required to estimate the mean properties of the dispersion and to predict when the hydrate particles are about to precipitate (Joshi, 2012). Assuming no slippage between the hydrate and the liquid – that is, $U_{LS} \approx U_{HS} \approx \tilde{U}_{LS}$ and $U_{LB} \approx U_{HB} \approx \tilde{U}_{LB}$ –, then the hydrate and water actual phase fractions become a function of their superficial velocities ratio (Shoham, 2006; Zerpa et al., 2013), Eqs. (11) and (12), respectively.

The pressure distribution is estimated by the momentum balance applied to the control volume of Fig. 2b, Eq. (13). The momentum variation inside the unit cell is neglected and the momentum fluxes crossing the unit cell borders are considered equal (Taitel and Barnea, 1990). Thus, the momentum balance turns into a force balance between pressure drop and friction. The friction is a combination of: (i) the friction between the wall and the unit cell structures (that is, the slug, the elongated bubble and the film); (ii) the interfacial friction between the gas and the liquid; and (iii) the head loss due to the recirculation at the bubble rear, in the wake zone (Cook and Behnia, 2000).

The energy balance, when applied to the control volume of Fig. 2c, gives rise to an expression for the mixture temperature distribution along the pipe, Eq. (14). Equations (15) to (17) are defined parameters that take the following phenomena into account: (i) the convection heat transfer in the slug and in the film, separately; (ii) the heat transfer with the external medium; (iii) the heat transfer between two consecutive unit cells, also known as *thermal scooping phenomenon* (Bassani et al., 2016b) and defined by the terms in Eqs. (18) and (19); and (iv) the heat generation due to hydrate formation. The radial thermal circuit of the system is used to correlate the wall temperature to the external medium temperature – that is, the given boundary condition –, Eqs. (20) and (21).

Finally, the term inside the exponential of the temperature distribution, Eq. (14), can be correlated to the heat transfer coefficient, Eq. (22), by using the mixture mass flow rate, Eq. (23).

4. SOLUTION METHOD

The pressure and temperature distributions, Eqs. (13) and (14), are used to estimate the pressure and temperature variations between two consecutive nodes as:

$$P_{(n+1)} = P_{(n)} - \left[\frac{\tilde{\tau}_{LS} S_{LS}}{A} \frac{L_S}{L_U} + \frac{\left(\tilde{\tau}_{LB} S_{LB} + \tau_{GB} S_{GB} + \tau_i S_i \right)}{A} \frac{L_B}{L_U} + K \tilde{\rho}_{LB} \frac{\left(\tilde{U}_{LB} - U_T \right)^2}{2 L_U} \right] \Delta z \tag{24}$$

$$T_{(n+1)} = \frac{p}{n} + \left(T_{(n)} - \frac{p}{n} \right) \exp\left(-\frac{n}{m} \Delta z \right) \tag{25}$$

where (n) and ($n+1$) indicate the current and the subsequent node, respectively, and Δz is the spacing between nodes. The evaluation of the RHS terms of Eqs. (24) and (25) follow an *Upwind Differencing Scheme*; therefore, all those terms are evaluated in node (n) so that the pressure and the temperature in node ($n+1$) can be found.

Equations (8) to (10) are used to correct the superficial velocities of the phases node by node. With the aid of Eqs. (24) and (25), the gas-liquid-solid slug flows with heat transfer and hydrate formation are fully characterized. The parameters belonging to these equations are evaluated as shown in Tab. 1.

The model was implemented as a procedural code using *Fortran90* language. The density of the hydrate-in-water dispersion was evaluated via an homogeneous model (Shoham, 2006) using the mean volumetric fractions of the phases, whereas the dispersion viscosity was evaluated according to Krieger and Dougherty (1959). The friction factors and the heat transfer coefficients of the unit cell structures were evaluated by Blasius and Gnielinski correlations respectively (apud Incropera et al., 2007). The hydrate temperature equilibrium was evaluated via *CSMGem*® software. The hydrate properties used for methane hydrates came from Jung et al. (2010). The gas (methane) is treated as Setzmann and Wagner (1991). The gas (methane) and liquid (water) properties were evaluated via *EES*® software.

5. RESULTS AND DISCUSSIONS

The objective of the present work is to evidence the importance of taking into account heat transfer and hydrate formation when simulating slug flows in long distance pipelines. To accomplish that, a simulation for a methane-water mixture flowing along a 1.5-km length 26-mm ID pipeline was chosen. The input data for the simulations are specified in Tab. 2. Three simulation cases were run: (i) an isothermal case, that is, analogous to the majority of the slug flow models found in the literature; (ii) a heat transfer case, the minority of the slug flow models found on literature; and (iii) a case with hydrate formation (also with heat transfer), scarcely found in the literature. The isothermal case is run by setting the inlet temperature equal to the external one, $T_{in} = T_{ext} = 298K$. For the cases where there is no hydrate formation, the results of Eqs. (1) to (3) were set as zero.

Table 2. Input simulation data.

Pipe length / ID / width	1.5 km / 26 mm / 1 mm
Pipe inclination	Horizontal
Pipe conductivity	30 W/(m·K)
Gas superficial velocity	1 m/s
Liquid superficial velocity	1 m/s
Fluids	CH_4 / H_2O
Pressure at the inlet	10 MPa
Temperature at the inlet	298 K (25°C)
External medium temperature*	277 K (4 °C)
External medium heat transfer coefficient	100 W/(m²·K)

*For the isothermal case, $T_{in} = T_{ext} = 298K$.

Figure 3a presents the mixture temperature distribution along the pipeline. For the isothermal case the temperature remains constant, as expected. For the heat transfer case, the mixture cools down showing an exponential trend characteristic of constant external temperature boundary conditions. When hydrate formation is considered, the mixture temperature crosses the hydrate equilibrium curve (red dashed line) at $z \approx 400$ m, but the critical subcooling is not reached until $z \approx 700$ m. At this point, the activation energy to nucleate the first hydrate particles is reached. The hydrate nucleation generates heat, thus reheating the mixture. At $z \approx 800$ m, the mixture converges to a nearly constant subcooling, relative to the hydrate equilibrium temperature. This subcooling results from the competition between the external medium cooling rate and the heat generation rate due to hydrate formation. This phenomenon is known as *heat transfer limitation* (Davies, 2009; Sloan et al., 2011).

Figure 3b presents the mixture pressure distribution along the pipeline. Pressure does not presented sensitivity for the three simulated cases. When heat transfer is considered, the pressure gradient slightly increases due to the mixture cooling and the consequent liquid viscosification – remembering that the liquid is the predominant in the momentum balance. Should an oil phase be considered, this mechanism is expected to become more important. When the hydrate formation is considered, the pressure gradient remained nearly constant. There are three main mechanisms affecting pressure drop when hydrates form: (i) the dispersion viscosification and a consequent pressure drop increase; (ii) the mixture slowdown due to gas consumption, with consequent shear stresses and pressure drop reduction (to be discussed in Fig. 3c); and (iii) the fact that hydrates may deposit at some point, thus reducing the cross sectional area and increasing pressure drop. The present model does not take (iii) into account, which is probably the dominant mechanism and may happen for hydrate volumetric fractions above 13% (Joshi, 2012). Thus, for the simulated case, mechanisms (i) and (ii) cancel out and then pressure drop is not sensitive to hydrate formation.

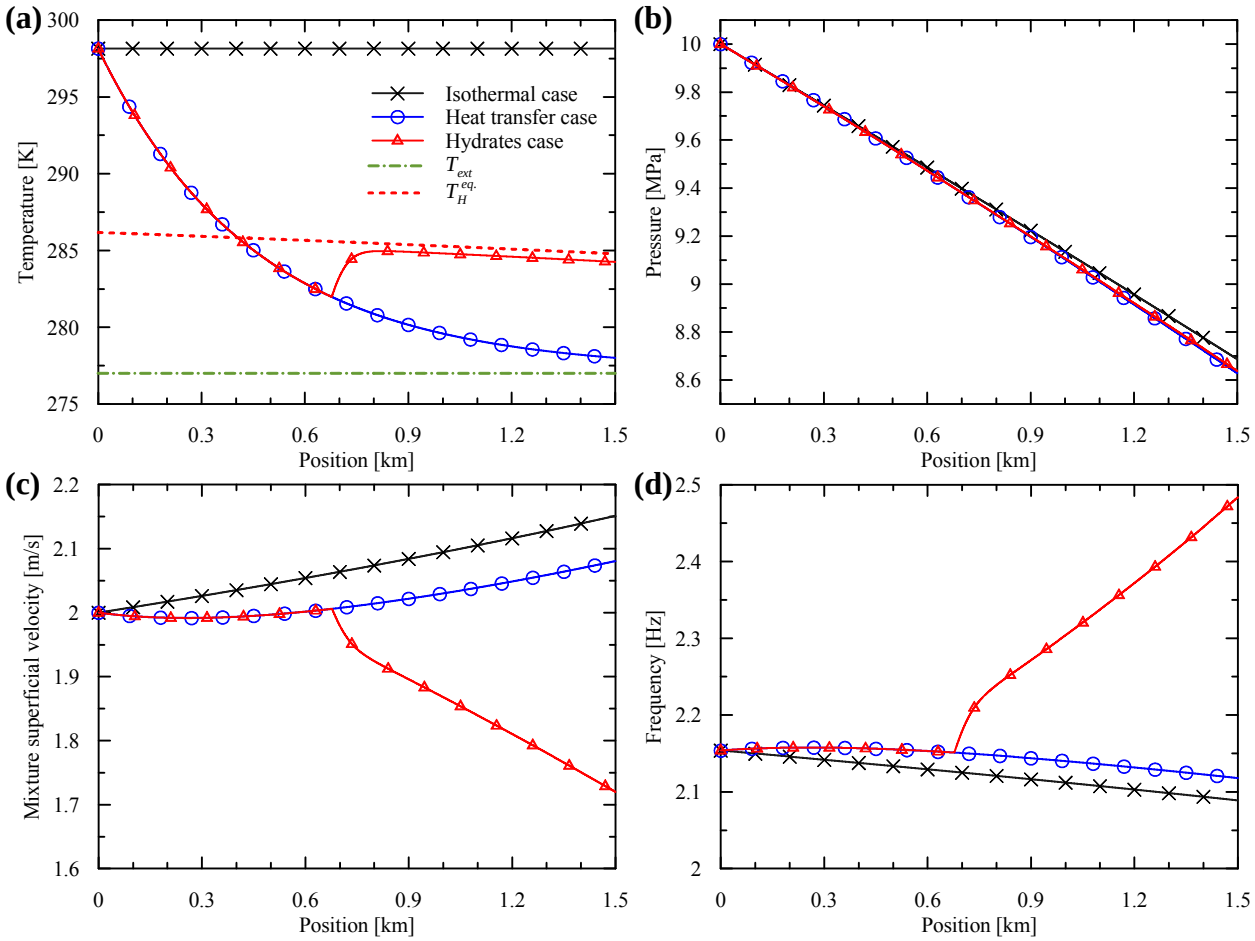

Figure 3. Results for: a) temperature, b) pressure, c) mixture superficial velocity and d) slug flow frequency.

Figure 3c presents the mixture superficial velocity distribution along the pipeline. For the isothermal case, the mixture velocity tends to increase along the pipeline, since the gas expands. When heat transfer is considered, the gas contraction due to the mixture cooling is competitive to the aforementioned mechanism, especially in the first half of the pipeline, where the temperature gradient between the mixture and the external medium is higher. When hydrate formation is considered, the mixture undergoes a slowdown due to gas consumption (a phase with high specific volume) to form the hydrate (a phase with low specific volume). That is, a mixture volume contraction takes place, herein related to the mixture slowdown since the system is open (there would be a pressure drop related to this volume decrease if the system were closed).

Figure 3d presents the slug flow frequency distribution along the pipeline. The slug flow frequency slightly decreases along the pipeline when the flow is isothermal. This is related to the gas expansion and a consequent no-slip liquid loading decrease, that is, the ratio between the liquid and the mixture superficial velocities j_L / J, which is directly proportional to the slug flow frequency (Gregory and Scott, 1969). When heat transfer is considered, the liquid viscosification due to temperature drop is reflected into a frequency increase (Schulkes, 2011). When hydrates form, the slug flow frequency presents a considerable augmentation, related to: (i) the dispersion viscosification and (ii) the no-slip dispersion loading increase (since gas volume is consumed, while the dispersion volume remains nearly the same because the hydrate formation and the water consumption rates almost cancel out).

Figure 4 presents the unit cell geometry in the pipe inlet and outlet. At the pipe inlet (Fig. 4a), all the three simulation cases are equal – since the input data is the same. At the pipe outlet (Fig. 4a), that is, after 1.5 km, the differences that arise from considering heat transfer and hydrate formation are remarkable. For the isothermal case, the unit cell and the elongated bubble lengths increase due to the gas expansion, whereas the slug remains with an approximately constant length. For the heat transfer case, the unit cell length is slightly smaller due to the gas contraction. However, the liquid viscosification due to the temperature drop reflects into slender elongated bubbles (Mazza et al., 2010), thus the bubble length increases slightly whereas the slug length decreases, keeping the mass conservation inside the unit cell.

When hydrate formation is considered, the elongated bubble is the most slender of all due to the dispersion viscosification, an effect that is more intense than the liquid viscosification due to the temperature drop. The elongated bubble and the unit cell reduce drastically in length due to the gas consumed to form the hydrate particles – that is, the mixture slowdown, Fig. 3c. This reduction can also be regarded as a consequence of the slug flow frequency increase after the hydrate nucleation, Fig. 3d. Finally, the slug length increases slightly when hydrate forms, due to the aforementioned increase in the non-slip liquid loading.

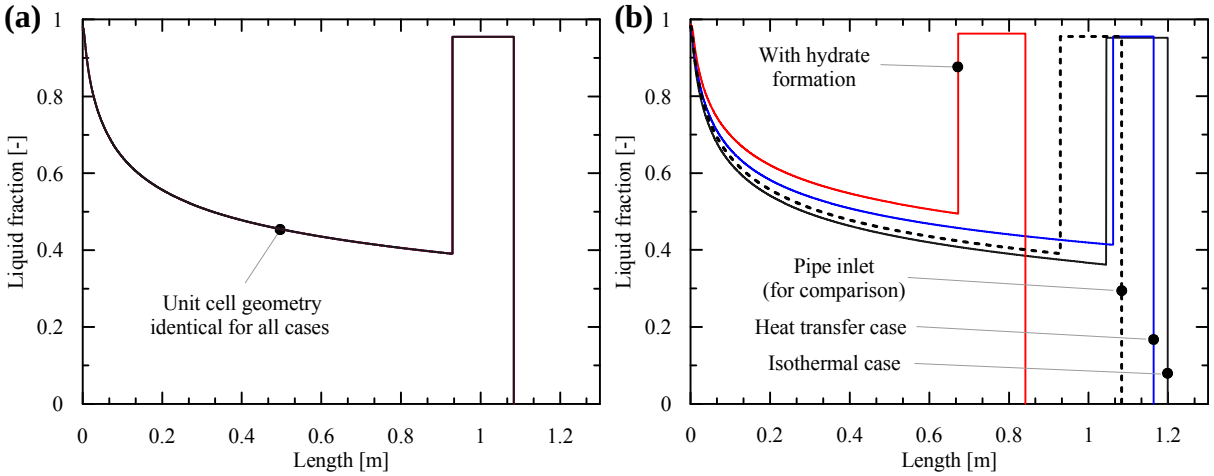

Figure 4. Unit cell geometry at the pipe: a) inlet and b) outlet.

6. CONCLUSIONS

The present work used a mechanistic model for predicting the effects of heat transfer and hydrate formation on the hydrodynamics of gas-liquid horizontal slug flows. The temperature distribution is dictated by the competition between the heat generation due to hydrate formation and the external medium cooling rate. The mixture superficial velocity depends on the competition between the gas expansion due to pressure drop, the gas contraction due to temperature drop and the gas consumption due to hydrate formation. The slug flow frequency is directly proportional to the liquid viscosity and to the no-slip liquid loading, and the three increase when hydrates form. The unit cell and the elongated bubble lengths tend to increase when hydrate formation is not considered, whereas the slug length reduces. The opposite occurs when hydrates are allowed to form. The liquid viscosification due to temperature drop and due to a dispersion formation is related to slender elongated bubbles.

7. ACKNOWLEDGEMENTS

The authors acknowledge the financial support of ANP and FINEP through the Human Resources Program for Oil and Gas Segment PRH-ANP (PRH 10-UTFPR), TE/CENPES/PETROBRAS (0050.0068718.11.9) and the National Council for Scientific and Technological Development (CNPq).

8. REFERENCES

Andreussi, P., Bendiksen, K.H., Nydal, O.J., 1993. Void distribution in slug flow. Int. J. Multiph. Flow 19, 817–828. doi:10.1016/0301-9322(93)90045-V

Bassani, C.L., Barbuto, F.A.A., Morales, R.E.M., Sum, A.K., 2016a. An analysis of the coupled effects of mass transfer, slug flow hydrodynamics and heat transfer during hydrate formation using a quasi-stationary mechanistic model, in: Submitted at 10th North American Conference on Multiphase Technology. BHR Group, Banff/Canada.

Bassani, C.L., Pereira, F.H.G., Barbuto, F.A.A., Morales, R.E.M., 2016b. Modeling the scooping phenomenon for the heat transfer in liquid-gas horizontal slug flows. Appl. Therm. Eng. 98, 862–871. doi:10.1016/j.applthermaleng.2015.12.104

Cardoso, C.A.B.R., Gonçalves, M.A.L., Camargo, R.M.T., 2015. Design options for avoiding hydrates in deep offshore production. J. Chem. Eng. Data 60, 330–335. doi:dx.doi.org/10.1021/je500601f

Cook, M., Behnia, M., 2000. Pressure drop calculation and modelling of inclined intermittent gas-liquid flow. Chem. Eng. Sci. 55, 4699–4708. doi:10.1016/S0009-2509(00)00065-8

Danielson, T., 2011. A simple model for hydrodynamic slug flow, in: Offshore Technology Conference. Offshore Technology Conference, Houston, USA. doi:10.4043/21255-MS

Davies, S.R., 2009. The role of transport resistances in the formation and remediation of hydrate plugs. PhD Thesis, Colorado School of Mines, Golden, USA.

Gregory, G.A., Scott, D.S., 1969. Correlation of liquid slug velocity and frequency in horizontal cocurrent gas-liquid slug flow. AIChE J. 15, 933–935. doi:10.1002/aic.690150623

Harmathy, T.Z., 1960. Velocity of large drops and bubbles in media of infinite or restricted extent. AIChE J. 6, 281–288. doi:10.1002/aic.690060222

Incropera, F.P., DeWitt, D.P., Bergman, T.L., Lavine, A.S., 2007. Fundamentals of Heat and Mass Transfer, Water. doi:10.1016/j.applthermaleng.2011.03.022

Issa, R.I., Kempf, M.H.W., 2003. Simulation of slug flow in horizontal and nearly horizontal pipes with the two-fluid model. Int. J. Multiph. Flow 29, 69–95. doi:10.1016/s0301-9322(02)00127-1

Joshi, S. V, 2012. Experimental investigation and modeling of gas hydrate formation in high water cut producing oil pipelines. PhD Thesis, Colorado School of Mines, Golden, USA.

Jung, J.W., Espinoza, D.N., Santamarina, J.C., 2010. Properties and phenomena relevant to CH4-CO2 replacement in hydrate-bearing sediments. J. Geophys. Res. Solid Earth 115. doi:10.1029/2009JB000812

Kjeldby, T.K., Henkes, R. a W.M., Nydal, O.J., 2013. Lagrangian slug flow modeling and sensitivity on hydrodynamic slug initiation methods in a severe slugging case. Int. J. Multiph. Flow 53, 29–39. doi:10.1016/j.ijmultiphaseflow.2013.01.002

Krieger, I.M., Dougherty, T.J., 1959. A mechanism for non-newtonian flow in suspensions of rigid spheres. Trans. Soc. Rheol. 3, 137–152.

Matthews, P.N., Notz, P.K., Widener, M.W., Prukop, G., 2000. Flow Loop Experiments Determine Hydrate Plugging Tendencies in the Field. Ann. N. Y. Acad. Sci. 912, 330–338. doi:10.1111/j.1749-6632.2000.tb06787.x

Mazza, R.A., Rosa, E.S., Yoshizawa, C.J., 2010. Analyses of liquid film models applied to horizontal and near horizontal gas-liquid slug flows. Chem. Eng. Sci. 65, 3876–3892. doi:10.1016/j.ces.2010.03.035

Medina, C.D.P., Bassani, C.L., Cozin, C., Barbuto, F.A.A., Junqueira, S.L.M., Morales, R.E.M., 2015. Numerical simulation of the heat transfer in fully developed horizontal two-phase slug flows using a slug tracking method. Int. J. Therm. Sci. 88, 258–266. doi:10.1016/j.ijthermalsci.2014.05.007

Nydal, O.J., Banerjee, S., 1996. Dynamic slug tracking simulations for gas-liquid flow in pipelines. Chem. Eng. Commun. 141, 13–39. doi:10.1080/00986449608936408

Petalas, N., Aziz, K., 1998. A mechanistic model for multiphase flow in pipes, in: Annual Technical Meeting. Petroleum Society of Canada, Calgary, Canada. doi:10.2118/98-39

Schulkes, R., 2011. Slug frequencies revisited, in: 15th International Conference on Multiphase Production Technology. BHR Group, Cannes, France, pp. 311–325.

Setzmann, U., Wagner, W., 1991. A New Equation of State and Tables of Thermodynamic Properties for Methane Covering the Range from the Melting Line to 625 K at Pressures up to 1000 MPa. J. Phys. Chem. Ref. Data 20, 1061–1155. doi:10.1063/1.555898

Shoham, O., 2006. Mechanistic modeling of gas-liquid two-phase flow in pipes, 1st ed. Society of Petroleum Engineers, Richardson, USA.

Simões, E.F., Carneiro, J.N.E., Nieckele, A.O., 2014. Numerical prediction of non-boiling heat transfer in horizontal stratified and slug flow by the two-fluid model. Int. J. Heat Fluid Flow 47, 135–145. doi:10.1016/j.ijheatfluidflow.2014.03.005

Sloan, D., Koh, C., Sum, A.K., 2011. Natural gas hydrates in flow assurance, 1st ed. Elsevier Inc., Burlington, USA.

Sloan, E.D., Koh, C.A., 2008. Clathrate hydrates of natural gases, 3rd ed. Taylor & Francis Group, Boca Raton, USA.

Taitel, Y., Barnea, D., 1998. Effect of gas compressibility on a slug tracking model. Chem. Eng. Sci. 53, 2089–2097. doi:10.1016/S0009-2509(98)00007-4

Taitel, Y., Barnea, D., 1990. A consistent approach for calculating pressure drop in inclined slug flow. Chem. Eng. Sci. 45, 1199–1206. doi:10.1016/0009-2509(90)87113-7

Turner, D.J., 2005. Clathrate hydrate formation in water-in-oil dispersions. PhD Thesis, Colorado School of Mines, Golden/CO, USA.

Zerpa, L.E., Rao, I., Aman, Z.M., Danielson, T.J., Koh, C.A., Sloan, E.D., Sum, A.K., 2013. Multiphase flow modeling of gas hydrates with a simple hydrodynamic slug flow model. Chem. Eng. Sci. 99, 298–304. doi:10.1016/j.ces.2013.06.016

9. RESPONSIBILITY NOTICE

The authors are the only responsible for the printed material included in this paper.